

## Detection Capability of an Advanced IR Technique for Wall-Thinning Defects in Nuclear Piping Components

Jin Weon Kim<sup>a\*</sup>, Sung Jae Jung<sup>a</sup>, Kyung Won Yun<sup>b</sup>, and Kyeong Suk Kim<sup>b</sup>

<sup>a</sup>Department of Nuclear Engineering, Chosun Univ., 375 Seosuk-dong, Dong-gu, Gwangju, Korea

<sup>b</sup>Department of Mechanical Design Engineering, Chosun Univ., 375 Seosuk-dong, Dong-gu, Gwangju, Korea

\*Corresponding author: jwkim@chosun.ac.kr

### 1. Introduction

The management of wall-thinning defects in piping components of nuclear power plants (NPPs) has become an important issue [1]. A key factor in the safe management of wall-thinning defects is reliable monitoring of the wall thickness of piping components. Accordingly, various thickness-monitoring methods for wall-thinning defects have been proposed [2-4]. One of these is infrared (IR) thermography. Our previous study investigated the applicability of an active IR thermography for detecting wall-thinning defects in nuclear piping components. It was seen that, aside from very short and narrow defects, common active IR thermography was able to detect all wall-thinning defects with depth  $d/t \geq 0.5$  in a pipe [5]. However, wall-thinning defects with depth  $d/t = 0.25$  could only be indicated from the thermal images when they had suitable lengths and circumferential angles.

An advanced IR thermography technique, so called lock-in method, has been developed and employed to improve the detection capability of defects in materials with high thermal conductivity [6]. It showed lock-in method provides better detection capability than common active IR thermography. Therefore, the present study conducted IR thermography tests employing lock-in method on pipe specimens used in the previous study. By comparing the resultant images of defects with those obtained from common active IR thermography, the detection capability of advanced IR thermography technique for detecting wall-thinning defects in piping components was investigated.

### 2. Experimental Procedure

#### 2.1 Pipe specimens

Six pipe specimens (S2-1~S2-4, S2-5, and S3-3) with artificial wall-thinning defects were used in the experiments. The specimens were made of Schedule 80 pipe sections with diameters of 2.5 and 4.0 inches, and the pipe material was carbon steel meeting the ASTM A106 Gr. B, commonly used in the secondary piping systems of NPPs. The length and diameter of S2-1~S2-4 specimens were 500mm and 113mm, respectively. Also, the length ( $l$ ) and diameter ( $D_o$ ) were 1200mm and 113mm for S2-5 and 700mm and 72.5mm for S3-3, respectively. All pipe specimens had artificial wall-thinning defects of various dimensions on both sides of the pipe, as shown in Fig. 1. The dimensions of wall-thinning defects were ranged from  $\theta/\pi = 0.0625$  to 0.25,

$L/D_o = 0.125$  to 1.0, and  $d/t = 0.25$  to 0.75. The axial and circumferential shapes of the defects were rectangular for S2-1~S2-4 and S3-3 and trapezoidal for S2-5. That is, the defects in S2-5 specimen had a slant edge in axial and circumferential directions.

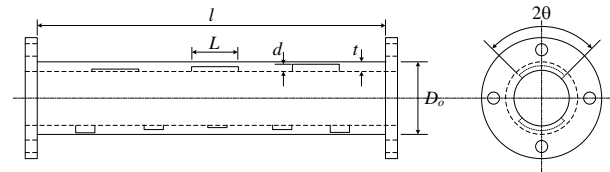


Fig. 1 Definition of geometries of pipe specimens and wall-thinning defects

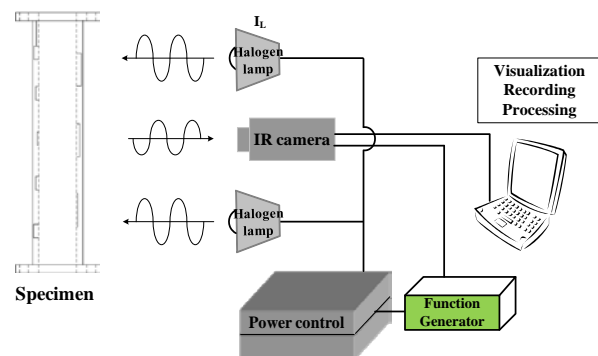


Fig. 2 Configuration of the IR thermography test using lock-in technique on the wall-thinned pipe specimens

#### 2.2 Test procedure

Lock-in IR thermography technique was used in the experiment. The test apparatus was composed of an IR camera (Silver 480), a thermal injection system, a function generator, and an image acquisition system. The thermal injection system consisted of two halogen lamps (1 kW per lamp) and a power controller. To apply lock-in technique, the specimens should be cyclically heated and the camera has to collect a series of thermal images at each cycle. Thus, the power controller and camera were synchronized using the sinusoidal function of the function generator. Phase images were calculated from the collected thermal images for each cycle by a software embedded in the image acquisition system. In this experiment, the frequency of heating cycle was set at 0.1 Hz. Figure 2 shows a schematic diagram of the test configuration.

### 3. Results and Discussion

Figure 3 comparatively presents the images of wall-

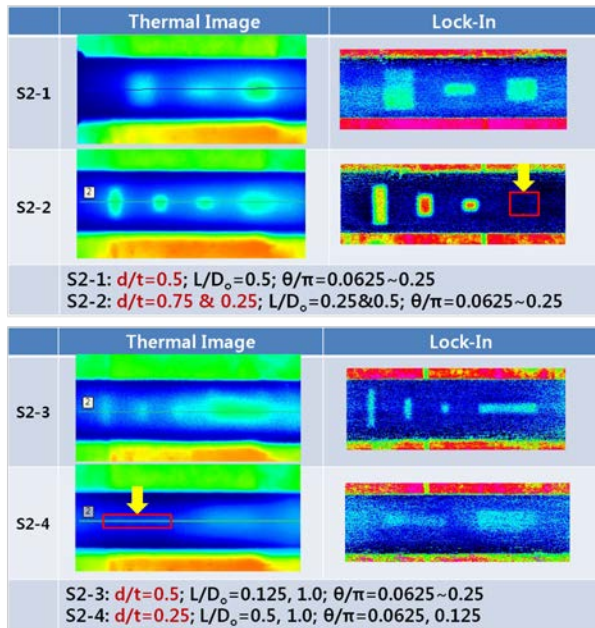


Fig. 3 Comparisons of defect images obtained from common and lock-in IR thermography tests for specimens of S2-1~S2-4

thinning defects from common active and lock-in IR thermography tests for S2-1~S2-4. Most of defects indicated by common active IR thermography were detected by lock-in IR thermography. Although the images were ambiguous, the lock-in IR thermography detected wall-thinning defects with a shallow depth ( $d/t=0.25$ ), which could not be detected by common active IR thermography (see S2-4). However, a defect with a shallow depth that was detected by common active IR thermography could not be detected by lock-in IR thermography (see S2-2). In this case, the improvement of detection capability by applying lock-in technique is not consistent. However, Figure 3 showed that the lock-in IR thermography provides more accurate dimensions of wall-thinning defect compared to common IR thermography for all defects. That is, rectangular shape of defects were well represented in the images from lock-in IR thermography. Therefore, it is seen that the capability in terms of sizing is improved by applying lock-in IR thermography technique. These characteristics were also observed at specimen of S3-3.

For wall-thinning defects with slant edge shown in Fig. 4, the images of defects obtained by common active IR thermography were not distinguished, whereas the images obtained by lock-in IR thermography were clearly distinguished. Also, the dimensions of defects with slant edge could be identified in the images obtained from lock-in IR thermography. In addition, lock-in IR thermography detected wall-thinning defects with a shallow depth, which were not indicated by common active IR thermography. Thus, it is seen that the applying lock-in technique improves the detection and sizing capabilities for wall-thinning defects with slant edge.

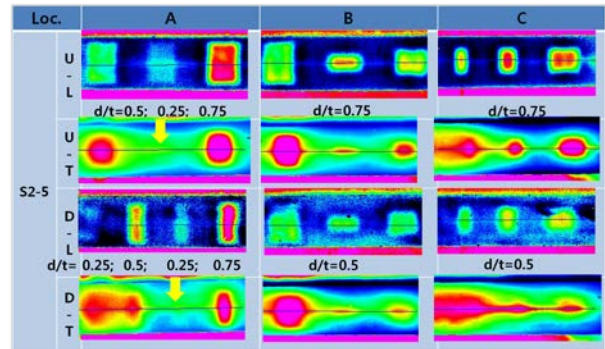


Fig. 4 Comparisons of defect images obtained by common and lock-in IR thermography tests for specimens of S2-2

#### 4. Conclusions

In this study, IR thermography tests employing lock-in technique were conducted on the pipe specimens with artificial wall-thinning defects. It showed that the applying lock-in technique improves the detection and sizing capabilities for wall-thinning defects in piping components. In particular, the improvement was clear for defects with slant edge.

#### Acknowledgement

This work was supported by the Nuclear Research and Development of the Korea Institute of Energy Technology Evaluation and Planning (KETEP) grant funded by the Korea Government Ministry of Knowledge and Economy.

#### REFERENCES

- [1] NRC Information Notice 2006-08: Secondary Piping Rupture at the Mihama Power Station in Japan, May 16, 2006.
- [2] Edalati, K. et al., 2006, "The use of radiography for thickness measurement and corrosion monitoring in pipes," Int. J. Press. Ves. Piping, Vol. 83, pp. 736-741.
- [3] Ryu, K.H. et al, 2008, "Screening method for piping wall loss by flow accelerated corrosion," Nucl. Eng. Design, Vol. 238, pp. 3263-3268.
- [4] Ammirato, F. and Zayicek, P., 1999, "Infrared thermography field application guide," EPRI/TR-107142.
- [5] Kim, J.W. et al., 2012, "Investigation of optimal thermal injection conditions and the capability of IR thermography for detecting wall-thinning defects in small-diameter piping components," Nucl. Eng. & Design (submitted)
- [6] Hung, Y.Y. et al., 2009, "Review and comparison of shearography and active thermography for nondestructive evaluation," Mat. Sci. Eng. Rep., Vol. 64, pp. 73-112.